University of Baghdad
College of Engineering
JOURNAL OF ENGINEERING

Journal of Engineering

journal homepage: www.jcoeng.edu.iq

Volume 31 Number 8 August 2025

Combining Terrestrial Laser Scanning and Drone-Based Photogrammetry towards Improving Volume Calculations in Construction Projects

Sharafaddin Th. Muhammed, **Fanar M. Abed**

Department of Surveying Engineering, College of Engineering, University of Baghdad, Baghdad, Iraq

ABSTRACT

This research aims to co-register UAV (Unmanned Aerial Vehicle) photogrammetry and Terrestrial Laser Scanning (TLS) for volumetric measurements of irregularly shaped material stacks available at construction sites in Iraq. The research investigates the potential of combining these techniques in comparison to standalone and traditional techniques to improve volume quantification and time consumption. An area containing a stockpile of bulk materials and building remnants was selected. A low-cost drone was used for data acquisition, whereas Structure from Motion (SFM) and Multi View Stereo (MVS) algorithms were used for processing and analysing the photogrammetric data. In contrast, Stonex X300 TLS device was used for laser data collection, while 3D Re-constructor software was used for data processing and analysis. The resulting volume from utilizing individual techniques came out as follows: 2692 m^3 from UAV photogrammetry with an accuracy of ±6 mm, 2730.99 m^3 from integrating photogrammetry and TLS with an accuracy of ±35 cm, while the conventional approach delivers 3048 m^3 with an accuracy of ±1.1 cm. The data integration (fusion) approach shows a high error level due to data registration obstacles, which can be overcome if the target-based registration approach is applied to increase the accuracy level to several millimeters. In this research, the results indicate the significant effectiveness of low-cost drones to deliver accurate volume measurements in photogrammetry, which outperform the conventional techniques for estimation, management, and precise volume calculation of the stocks and materials in construction projects. This was approved in the perspective of time, data intensity, cost effectiveness, and labor intensity following data analysis.

Keywords: Construction works, Volume calculations, Irregular stockpiles, UAV photogrammetry, Laser scanning.

1. INTRODUCTION

Handling, transportation and storage of large quantities of different materials is essential in many operations, as can be seen in various industries where bulk materials are used as

*Corresponding author
Peer review under the responsibility of University of Baghdad.
https://doi.org/10.31026/j.eng.2025.08.03

Article received: 04/10/2024
Article revised: 07/05/2025
Article accepted: 11/06/2025
Article published: 01/08/2025

inputs, outputs, or where they flow as money **(Tucci et al., 2019)**. The term "stockpile" usually means a large accumulation of stacked materials, such as mining deposits, the remains of buildings, and construction materials like gravel, sand, asphalt, trash, and big rocks **(Makhathini et al., 2023)**. They can be stored in reserve for future use when resources are low or need to be removed from the workspace **(Ajayi and Ajulo, 2021)**. There was an earlier time when volume monitoring and computation would be done with the aid of traditional surveying instruments such as Total Station and Global Navigation Satellite Systems (GNSS) **(Shen et al., 2019)**. Those methods still have their problems, such as time consumed for the survey, site security, accessibility, and costs are significantly higher, and measurements are possible only at a few characteristic points, which is not enough for a precise description of highly detailed complex shapes **(Tucci et al., 2019)**. Nowadays, an evolution that is getting more and more widespread among the methodologies of engineering is UAV photogrammetry. Besides topographic mapping and all other photogrammetric applications, UAVs are an ideal fit for mining engineering plus geodesy, and in particular volumetric computation **(Raeva et al., 2016)**. Measurements conducted by traditional methods, using surveying equipment, can be highly accurate, but they are slow and demand a lot of labor; on the other hand, photogrammetric approaches can give details at a high level over large areas and could be completed within an hour **(Sang, 2020)**. It's important to mention that the laser scanning technique can be used to measure structures, landscapes, and archeological sites with a high level of precision. The data provided from laser scanning can be used in many different ways: developing 3D models, change monitoring, time variation, and providing virtual tours **(Cucchiaro et al., 2020 ; Abbas and Abed, 2024)** and of course volume calculation, which is the objective of this study. Hence, this study aims to assess the quality of volumetric computations by automatic remote sensing techniques (UAV, TLS), comparing the results obtained from each of them to assess the effectiveness and decide which technique is more appropriate for such applications (earthwork volume calculation).

Reviewing previous studies in volume calculations will be discussed in the coming paragraphs. In recent years, UAV photogrammetry has emerged as a viable way of measuring and calculating volume **(Deliry et al., 2021)**. In addition, laser scanning is another excellent approach that can be employed in volume computation. The use of high-resolution cameras in UAVs has become widespread, permitting thorough and accurate map production with only one flyover **(Turner et al., 2012)**. Based on earlier studies, it was discovered that the employment of UAV platforms and photogrammetric techniques for volume determination is a valuable and feasible approach **(Remondino, 2003)**. For example, one of the UAV photogrammetry studies for volume calculation is **(Yakar and Mutluoglu, 2010)** study, which conducted several experiments to determine the efficacy of close-range photogrammetry in the volume of objects. In a laboratory, an artificial conical object having a volume of 364.2 cm^3 was captured with a Sony digital camera. Volume calculations yielded (359.5 cm^3) and (359.7 cm^3) in Surfer and CAD, respectively. The author regarded a 1.28% error as substantial for practical purposes. The results presented here demonstrate that close-range photogrammetry is an effective method for estimating the amounts of materials utilized in various areas. It is very precise and efficient, thereby replacing traditional methods that may take longer or be more costly for no reason other than frustration **(Yakar et al., 2014)**.

Furthermore, A multi-copter UAV was used and compared with total station calculations in **(Arango and Morales, 2015)** study to estimate stockpile quantities. It was discovered that

the UAV approach provides a lower estimate of the volume than the total station method. The recorded volume disparity was 2.88% between the overall station predicted figure (11831.20 m^3) and the actual number (11500.00 m^3), but for the UAV, it was -0.67% between 11423.58 m3 and the genuine volume **(Arango and Morales, 2015)**.

In contrast, laser scanning has become so precise and rapid that it is widely employed for determining the quantity of stocks **(Slattery and Slattery, 2010)**. Laser scanners mounted to drones or ground-based platforms may swiftly and precisely evaluate the material volume in piles, such as sand, coal, or metals **(Nguyen and Quang, 2021)**.

For example, one of the laser scanning studies for volume calculation is **(Yakar et al., 2014)** who used TLS and close-range photogrammetry to compute the volume of excavation and filling areas. The volume obtained by employing TLS was (26.9256 m^3). This result was achieved by scanning the location in 2 cm intervals and aligning the model using control points with an accuracy of m_{xy} = ±1.2 mm and m_z = ±1.1 mm. Using the same control points to align the model, they obtained the volume from close-range photogrammetry, which was (25.0845 m^3). This study looked at the possible applications of TLS and close-range photogrammetry for volume calculations. TLS requires only one person to perform the survey. It may be put up in a safe position away from unstable mining zones and begin recording point cloud data at any increment necessary by the operation. When compared to close-range photogrammetry approaches, laser scanners produce faster and more accurate readings, but the cost of TLS is higher **(Yakar and Mutluoğlu, 2010)**.

Furthermore, **(Mabrur et al., 2023)** calculated the amount of supplies stored in a warehouse for sale. The volumetric technique is employed in the stockpile measuring procedure by using a laser scanner instrument. The fourth-quarter stockpile at the Adipala PLTU Coal Yard. According to the estimates, there were (121,420,574 m^3) of coal in the stockpile on the west side of the yard, and (88,230,355 m^3) on the east side. After estimating (209,650,929 m^3) coal using the bulk density of the survey data, (180,384,417 m^3) coal was produced. In conclusion, there are various advantages to adopting TLS, including faster and more precise measurements. It is clear that the point cloud findings may be a reference for predicting stockpile volume based on both planning and actual data **(Mabrur et al., 2023)**.

Following this, it turns out to be obvious that most construction sites that contain earth work and stockpiles in Iraq rely nowadays on the expensive and time-consuming traditional techniques to perform a quantity survey.

Therefore, in this study, it was aimed to prove the potential of remote sensing technologies in the field of quantity surveying works, especially for large and irregular shaped objects and stockpiles. Further, the research aims to address limitations in individual techniques and highlight the potential of integrating TLS and UAV photogrammetry to increase resolution and deliver high-end products in terms of precision and accuracy following co-registration algorithms.

2. STUDY AREA

The case study site for this research is shown in **Fig. 1**, which is a stockpile of soil and other piled materials such as concrete, metal, and rocks at an empty area in the University of Baghdad campus, situated within the borders of the College of Agricultural Science, AL-Jadrya, Baghdad. Its geographical position is 33°16'3.79"N from the equator and 44°22'39.63"E from the Greenwich meridian. The surveys and site measurements were taken between January and March 2022.

Figure 1. Study area location.

3. METHODOLOGY

Laser scanning and UAV photogrammetry are highly efficient techniques for surveying projects in terms of accuracy, precision, efficiency, speed, flexibility, cost-effectiveness, and even safety **(Kovanic et al., 2023)**. This study attempts to examine the quality of volume calculations using these two autonomous digital techniques. To achieve the study objectives, a preplanned methodology was applied for data collection, processing, data analysis, post-processing, validation, and measurements to quantify the achieved outputs as shown in **Fig. 2**.

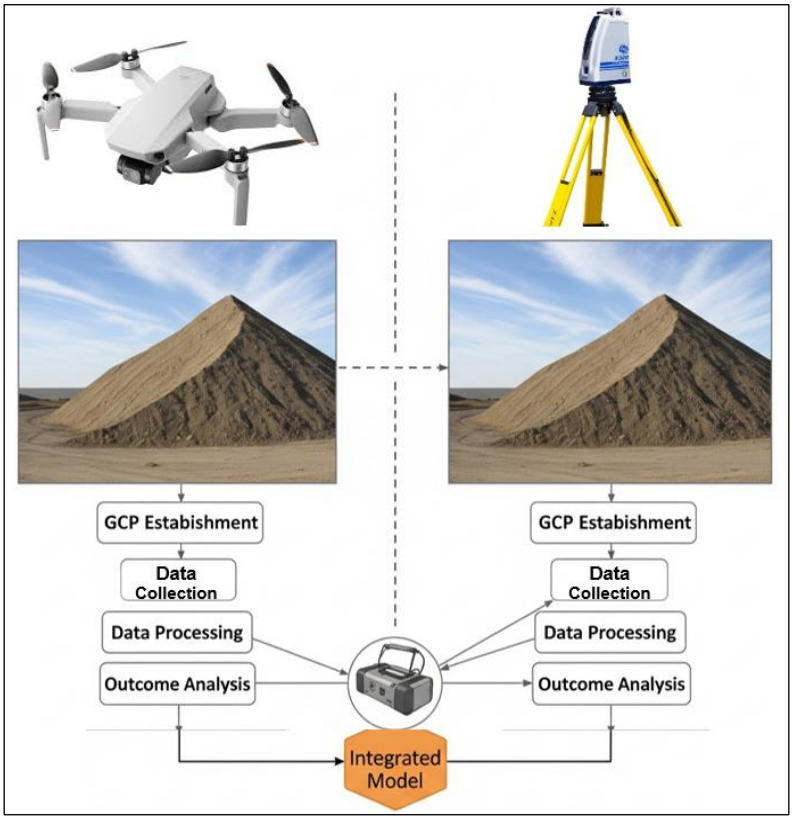

Figure 2. Research methodology workflow.

3.1 Materials

The materials to be employed in the research were determined by the extent to which they would help in the attainment of research objectives. These instruments include the

utilization of an appropriate low-cost UAV system (DJI Mini-2), a camera that is attached to the UAV for aerial photography with 12 megapixel resolution, a GPS system that is used to capture GCPs, and a Laser system (Stonex X-300) for scanning of the stockpile's surface with the finest resolution as shown in **Fig. 3**.

Figure 3. Instruments used in the study, (Left) DJI Mini-2 drone, (Right) Stonex X-300 laser scanner.

3.2 Data Acquisition and Processing from UAV Flight

The flight plan and picture acquisition parameters were set up on the drone-link website, see **Fig. 4** and then uploaded to the drone link mobile application, to begin the autonomous drone flying mission in the field and gather all of the stockpile data, see **Fig. 5**. All of the relevant parameters have been set and illustrated, as shown in **Table 1**.

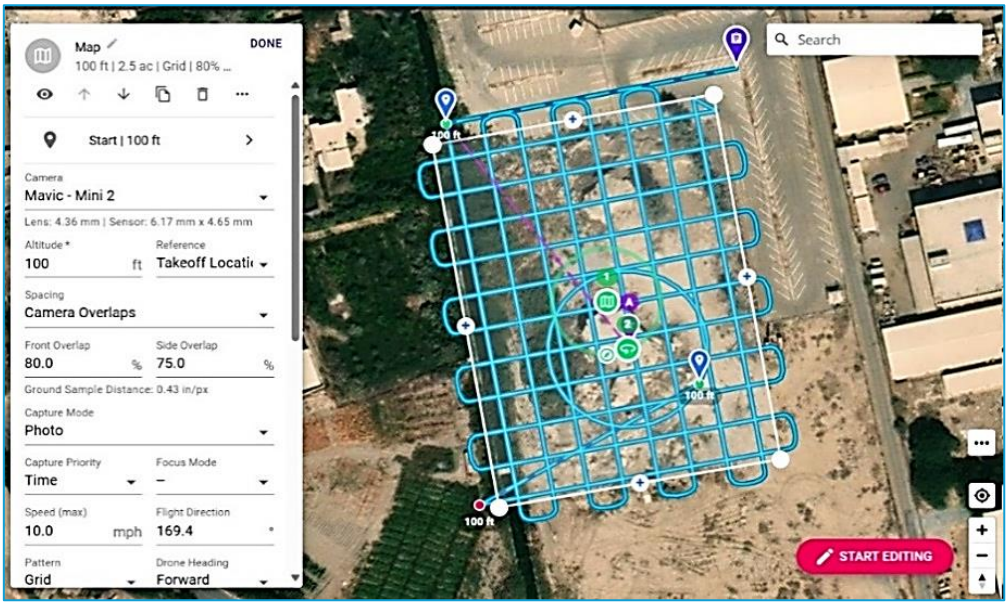

Figure 4. Flight plan settings in drone link website.

Figure 5. Flight progress and capturing of images by drone-link mobile application.

Table 1. Flight mission parameters and settings.

Parameter	Specifications
Number of images (TNI)	317
End lap and Side lap (PE and PS)	80% end lap & 75% side lap
Airbase (B)	8.94 m
Number of flight lines (NFL)	20
Flying Height	100 ft = 30 m
UAV speed	10 mph = 16.09 kmph
Capturing angle	-90 degree
Capturing interval	2 seconds
GSD (ground sample distance)	0.4 in/pix = 1 cm/pix
Camera type	DJI-mini-2 (12 M-pixels)
Camera specs.	Lens= 4.37mm, sensor= 6.17 mm x 4.65 mm
Flight time	14.57 minutes

The number of the flight lines and camera trajectories (pre-mission mentioned in **Table 1** are calculated and as shown in Eqs. (1-7) **(Noori et al., 2024)**:

$$W = w \times S \tag{1}$$

$$L = l \times S \tag{2}$$

$$SP = W \times ((100 - S_{Lap})/100) \tag{3}$$

$$NFL = \left(\frac{Width}{SP}\right) + 1 \tag{4}$$

$$B = L \times ((100 - F_{Lap})/100) \tag{5}$$

$$NIM = \left(\frac{Length}{B}\right) + 1 \tag{6}$$

$$Total\ number\ of\ images = NFL\ X\ NIM \tag{7}$$

Where (W) and (L) are the image ground coverage in image width (w) and image length (l), S is the scale number of the image, (SP) is the distance between flight lines, S_{Lap} is the amount of side lap, (NFL) is number of flight lines, Width, and Length are representing the

AOI dimensions on the ground, (B) is the distance between consecutive images (Airbase), F_{Lap} is the forward lap amount, and (NIM) represent the number of images per flight line. When the aircraft is moving at a speed (v) and two successive images are captured, then the time (t) between successive images becomes **(Lai et al., 2010)**, see Eq. (8). It can be calculated and set for the entire mission as follows:

$$Time\ (t) = \frac{Airbase\ (B)}{Aircraft\ speed\ (v)} \tag{8}$$

Where (B) is the airbase, which equals 8.94m, and the (v) is the aircraft speed which was set at 10 mph (4.47 m/s), then the time was computed to be 2 seconds.
The obtained photos were processed using the software Agi-soft Meta Shape; after the images were loaded, a number of operations were performed to adjust the photographs' position **(Viola and Jones, 2004)**. Initially, the exposure positions were roughly correct when compared to the accuracy of GCPs. However, this is only the first step in achieving positional precision down to millimeters. To reduce inaccuracies, the extracted 3D model is corrected and georeferenced by applying aerial triangulation and affine transformations **(Erzaij and Obaid, 2017; Wu et al., 2018)**. **Fig. 6** illustrates UAV photogrammetry methodology.

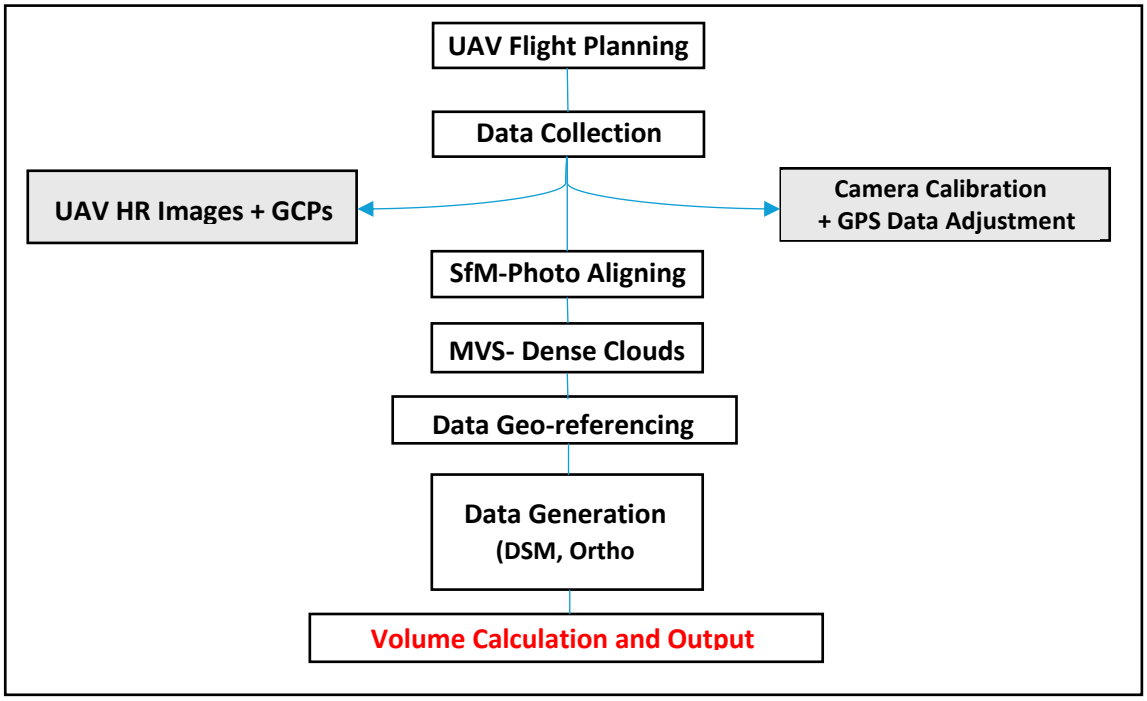

Figure 6. Workflow of the UAV photogrammetric methodology.

For georeferencing and other surveying operations, 9 ground control points were measured using GNSS technology, according to **(Yakar and Mutluoğlu, 2010)** suggests the use of no fewer than four GCPs in each module for photogrammetric operations. GCPs increase the relative alignment and geographic accuracy of the tie-point-based model. The first point was measured using a Topcon-Gr-5 receiver in static mode for two hours, while the others were measured in real-time kinematic (RTK) mode. The ground targets used for the

measurements contained a 60×60 centimeter black and white wooden plate that represented the control locations, as shown in **Fig. 7**.

Figure 7. Ground control points, (Left) GCPs targets, (Right) distribution of the points in the site (the green points are measured in RTK mode while the red colored are measured in static mode).

In this study, UAV photos were aligned, and the orientation parameters were determined using SFM algorithms. The photos were then geotagged and linked to the GCPs coordinates to calibrate the camera (Photos) location via internal, relative, and absolute orientation. Finally, aerial triangulation is carried out using Bundle Adjustment (BA), and the Multi-View-Stereo (MVS) technique was applied to provide rectified and georeferenced 3D point cloud. The overall point cloud accuracy depends on the checkpoints' accuracy **(Venkataraman and Pinto, 2008)**, which was 7 mm, as shown in **Table 2**.

Table 2. The quality report details errors for ground control points (GCPs) and checkpoints (CP) (highlighted in red) in millimeters, along with image re-projection errors in pixels.

Label	X error (mm)	Y error (mm)	Z error (mm)	Total Error (mm)	Images (pix)
GCP9	7.4306	3.33951	-3.21149	8.7567	0.092
GCP1	0.822865	5.70783	4.75156	7.4722	0.123
GCP2	4.34601	2.05176	-1.32042	4.98408	0.006
GCP3	1.23234	-3.8487	-4.64249	6.15499	0.166
CP4	-2.05619	5.58763	6.30453	8.6716	0.212
CP5	-4.83715	1.59342	0.192419	5.09648	0.177
GCP6	3.07495	-0.92691	-0.01903	3.21167	0.17
GCP7	-3.47992	-8.61333	-0.35295	9.29644	0.028
GCP8	1.91969	2.49726	0.82422	3.2559	0.142
Total (GCPs)	3.80878	4.53618	2.85336	6.57461	0.141
Total (CPs)	3.71658	4.10856	4.46005	7.11234	0.19

3.3 Data Acquisition and Processing Using Laser Scanning

The comprehensive laser scanning methodology, which includes data collection, registration, and post-processing, is illustrated in **Fig. 8,** and it will be explained in the next sections.

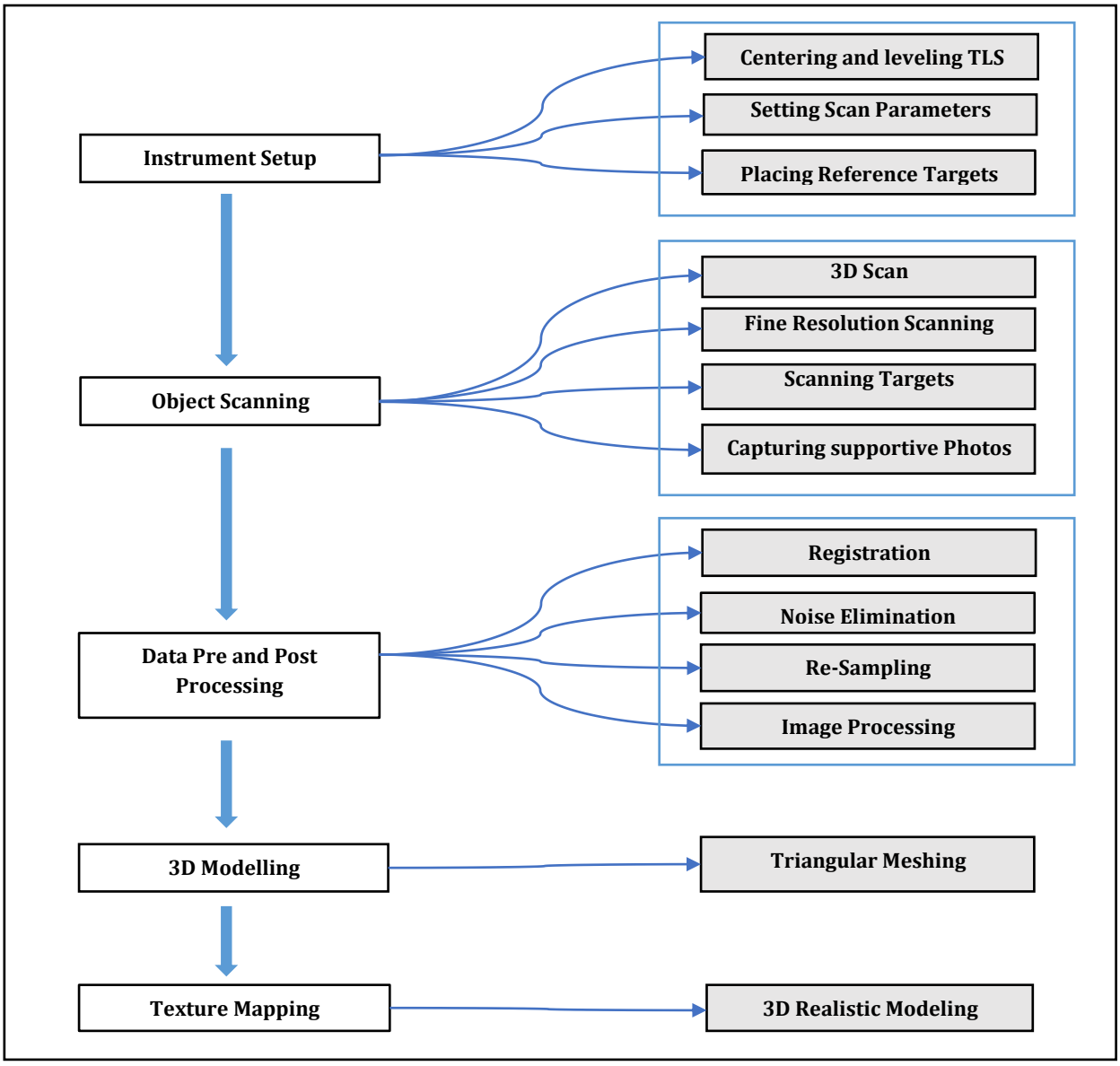

Figure 8. Laser scanning data collection and processing workflow.

Planning laser scanning projects is an essential step towards an adequate result **(Shanbari et al., 2016)**. it needs Careful consideration of a number of factors, including project objectives, target area identification, and appropriate laser scanning technology selection **(Evans et al., 2009)**, scanning strategy plan, control point establishment, safety considerations, and data processing and management plan development, are necessary to ensure the laser scanning project's successful implementation **(Rashidi et al., 2020)**. A well-defined scanning plan was set to include all parameters such as scanning density, scanning resolution, scanning range, scanning speed, laser intensity, field of view (FOV), and Scanning pattern. Scanning parameters are illustrated in **Table 3** and scanning stations in **Fig. 9**.

Table 3. Laser scanning parameters.

Parameter	Specifications
Scanning stations	13 stations
Field of view (FOV) (scan angle)	150̊ to 90̊
Scans overlap	From 60% to 50%
Scanning speed	0.007 m/s
Laser intensity	40,000 pt./s
Scanning resolution	Fine (highest resolution) 4x
Scanning pattern	oscillating mirror (jagged pattern)
Scanning density	39 × 39 mm at 100 m (12 × 12 mm at 30 meters)
Scanning range	From 20 to 15 meters

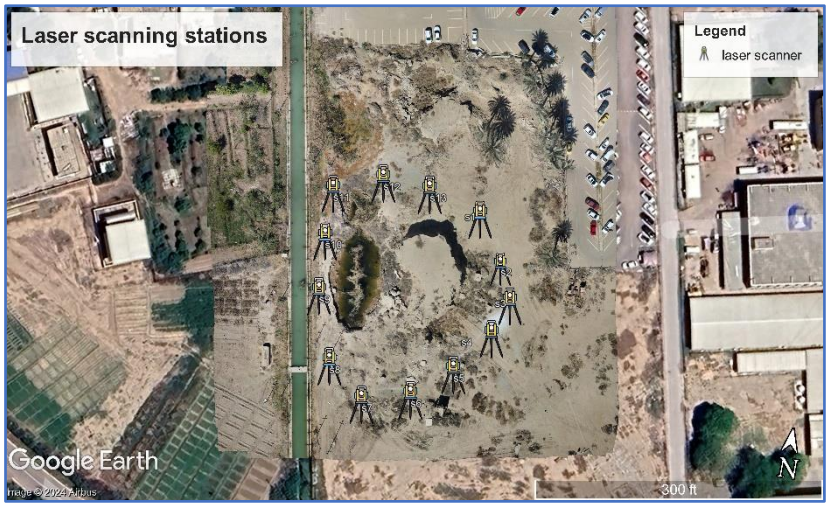

Figure 9. Laser scanning stations.

After data collection is complete, the first step in laser scanning data processing is the registration process **(Mohammed et al., 2015)**, which aligns several point clouds that were captured from different orientations and locations together **(Holz et al., 2015)**. Since a single scan can only provide a small field of view, registration is an essential step in data processing **(Salvi et al., 2007)**, see **Fig. 10** for several scans' registration.

Now, it's important to perform post-processing for laser scanning data, which is an essential action to do, encompassing point cloud refinement, data integration, model development, data visualization, and analysis (**Remondino, 2003)**. Point cloud refining is the process of reducing the number of points in the cloud while preserving crucial details, which can improve processing speed and minimize file size **(Alexiou et al., 2019)**. The laser scanning resulted in a point cloud number of (14,927,420) points for this study; however, following the refinement process, the number of points decreased to (4,728,430).

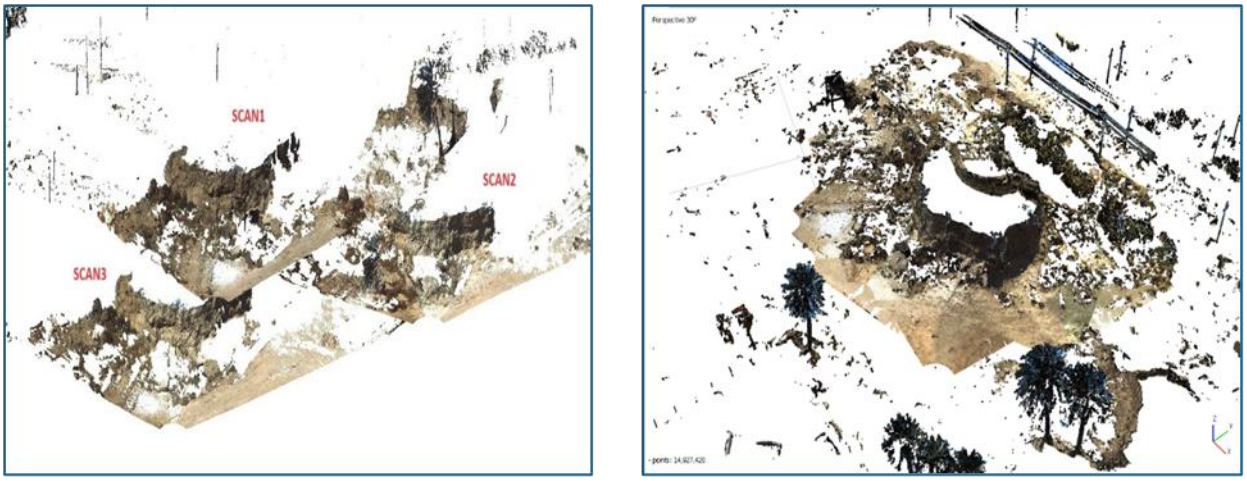

Figure 10. Registration of several scans, (Left) multiple randomly distributed scans, (Right) single registered scan (point cloud).

3.4 Data Integration Process

Combining data sets, such as laser scanning data with other data sources like photogrammetry data, is a sort of data integration that merges all the information acquired into a single data set **(Zhang, 2010)**. Additionally, it involves coordinate system conversion, which calls for converting the data into other coordinate systems using matrix transformations or geodetic coordinate conversion **(Janssen, 2009; Alkarawi et al., 2023)**. The integration process was used in this study to fill the gap in the laser data created at the top surface of the OOI. This gap was caused by inadequate coverage because of using a terrestrial laser scanning platform while the height of the AOI (stockpile) was around 7 meters. So, to provide an integrated dataset covering the full object, integration between UAV and TLS data was carried out. The process created a fused 3D point cloud model to close the gap created by LS and improve the resolution of the photogrammetric point clouds (863,971) points. In this stage, the OOI is fully covered, and the 3D point clouds' resolution is increased to (5,592,401) points; the accuracy of the integration process was (±0.35m). **Fig. 11** illustrates the LS point clouds before and after the integration process.

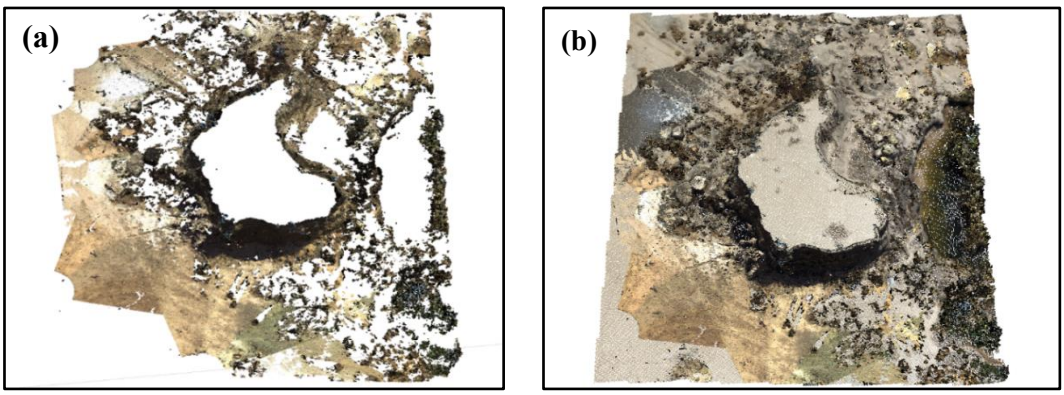

Figure 11. Integration process, (a) TLS point cloud before integration, (b) point cloud after integration process (TLS+UAV).

3.5 Volume Calculation

The primary objective of this study is to examine the quality of volume computations resulting from advanced digital techniques (i.e., UAV photogrammetry and laser scanning). To ensure a fair analysis, it is necessary to employ the same volume calculation technique and software, which is AutoCAD civil 3D. Several methods are used in civil engineering and land surveying to calculate earthwork volumes and manage excavation and fill operations, such as the Grid method, Triangulated irregular network (TIN) method, Average end area method, Prismoid method, and Mass haul diagram method. In this study, the TIN method was adopted, which is a common and exceptional method used within Civil 3D software. This approach ensures the accuracy of predicting material quantities to be carried between two surfaces **(Lukacevic and Füssl, 2014)**. The TIN volume method was employed by producing two surfaces from the acquired data in the field by using each of UAV photogrammetry and TLS techniques, as shown in **Fig. 12.**

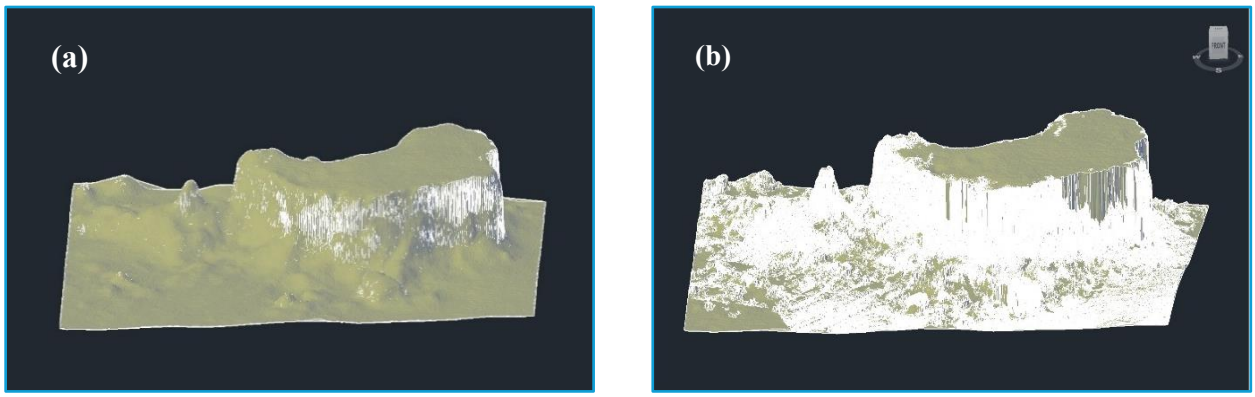

Figure 12. Objects generated surfaces in Civil 3D, (a) surfaces created from UAV Photogrammetric data, (b) surfaces created from fused UAV+TLS data.

The mathematical formula used for volume calculation in AutoCAD Civil 3D is called Prismoidal Formula. The Prismoidal formula is a way of calculating the volume of a prism-like shape (or any component of it) based on the cross-sectional areas **(Malvić et al., 2014)**. It is especially effective for volumes that may be roughly represented by a succession of frustums, which are fragmented pyramids or cones.

The Prismoidal formula is expressed in Eq. (9) **(Viola and Jones, 2004)**:

$$V = \frac{L}{6}.(A1 + 4A_m + A2) \quad (9)$$

Where:
V is the volume of the prismoid, L is the height of the prismoid (the distance between the two parallel bases, A_1 is the area of the first base (cross-section), A_2 is the area of the second base (cross-section), A_m is the area of the mid-section (the cross-sectional area at the midpoint between the two bases)

4. RESULTS AND DISCUSSION

This section discusses and analyzes the volume quantification outcomes that were produced using UAV photogrammetry and a combined RS data approach based on co-registering photogrammetry and TLS innovative techniques. It demonstrates the difference between individual scenarios from the perspective of data intensity, time consumption, and cost by providing stockpile volume quantification statistics following the methodology presented previously.

4.1 Quality of 3D Point Clouds

Individual scenarios followed in this study have produced 3D points in different quantities and accuracies. The UAV photogrammetry had resulted in (863,971) points of ±0.0065m accuracy based on CP checkpoint accuracy. It is important to mention that photogrammetry can provide much denser data, but in this research, the photogrammetric data was subsampled to overcome the computer freezing issue acquired during data densification and depth information extraction in the photogrammetric workflow. This is usually acquired due to the low specifications of the computer hardware. However, data sub-sampling did not affect the geometric quality of the 3D point clouds as the data accuracy still the same. On the other hand, the TLS approach resulted in (5,592,401) point clouds to be later integrated with the photogrammetric data to complete the surface coverage with accuracy reaching ±0.35m following the co-registration process. **Fig. 13** shows the density of the photogrammetric data following the intensity geometric tool in CC. These points have been enlarged 6x times when integrated into TLS data following the data integration approach demonstrated in **Fig. 14**. However, the conventional approach delivers 3048 m^3 with an accuracy of ±1.1 cm.
One of the reasons behind the tremendous data density of the TLS technique is that laser devices are usually collecting data for volume quantifications using close ranging as devices sets in a closer range than UAVs, which are away from the ground and the OOI.

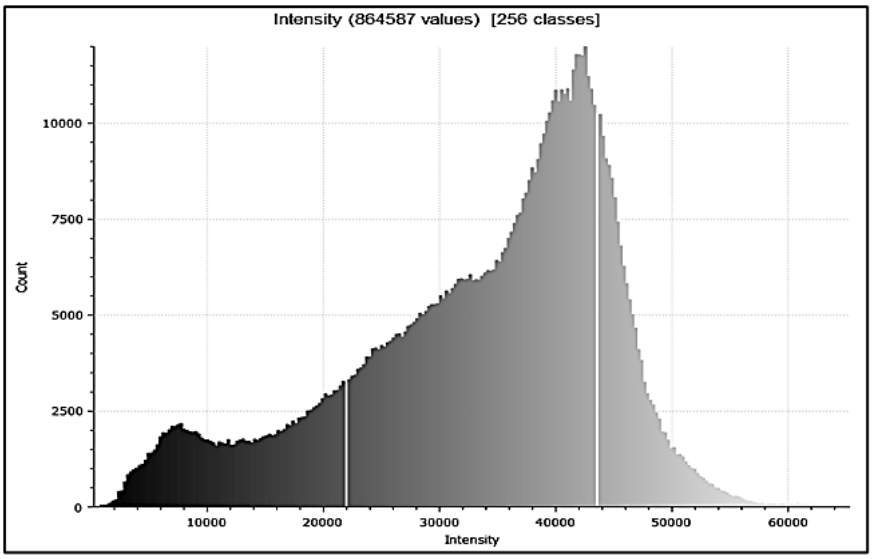

Figure 13. Histogram shows density of UAV photogrammetric dataset using intensity geometric analysis.

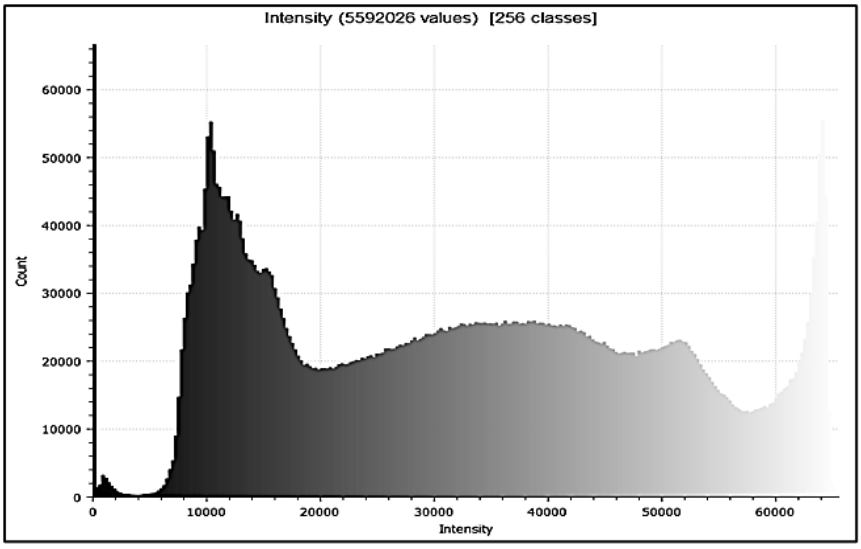

Figure 14. Histogram showing density of the integrated TLS and photogrammetric dataset using intensity geometric analysis.

4.2 Triangulated Irregular Network (TIN)

The accuracy of volume calculations mainly depends on the quality and density of data points that are used, as poor-quality data can cause errors. In this study, different numbers of points in different densities from individual techniques was acquired, which directly affects the overall density of the generated TIN surfaces. This is due to the fact that the TIN is generated from the closest 3 points to form a single triangle. See **Table 4** illustrating the number of TINS generated from photogrammetry, fused, and traditional approaches. The process of TIN surface generation and Prismoids (volume) surface creation is implemented in AutoCAD Civil 3D. **Fig. 15** shows TIN generated from individual techniques.

Table 4. The number of triangles (TIN) and Prismoids generated from individual techniques.

Category	UAV Photogrammetry	Fusion	Traditional
Points	863,971	5,592,401	258
Triangles	287,990	1,864,133	86
Prismoids	143,995	932,066	43

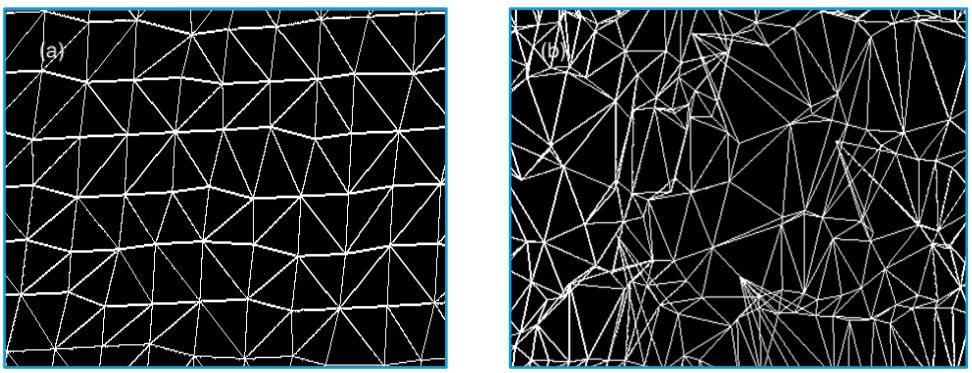

Figure 15. TIN generated from each technique, (a) TIN generated from UAV photogrammetry, (b) TIN of TLS+UAV photogrammetry.

From **Table 4**, it was obvious to notice the tremendous number of prismoids extracted from the data fusion approach and thereby outperform other approaches. The combination of TLS with photogrammetry improves prismoid extraction's precision, comprehensiveness, and dependability. When compared to employing photogrammetry alone.

Fig. 15 demonstrates the visual difference between the TIN models generated from individual techniques. The density of the fused TIN dataset is so high, but it can be noticed some randomly generated triangles that might affect the volume calculation process. This is due to the mitigation of the integration error between UAV point cloud and TLS point cloud obtained due to the co-registration scenario. In contrast, the TIN generated from UAV photogrammetry has medium density if compared to the fused TIN, however, the triangles are equally distributed in the model, which is preferable in the current case to represent the realism of the stockpile terrain.

4.3 Volume Quantification Analysis

4.3.1 Volume From UAV Photogrammetric Data

Within the UAV photogrammetry technique, the volume of the stockpile was computed and analyses in an individual routine to examine potentials and limitations. The process starts by importing the point cloud into AutoCAD Civil 3D and creating top and base surfaces for the OOI using surface creation tools. Later, the volume dashboard tool was used, and the surface comparison settings were applied. The volume bounded by the top and the base surfaces was computed to be (2692.39 m^3). **Fig. 16** shows the volume computation from the photogrammetric data.

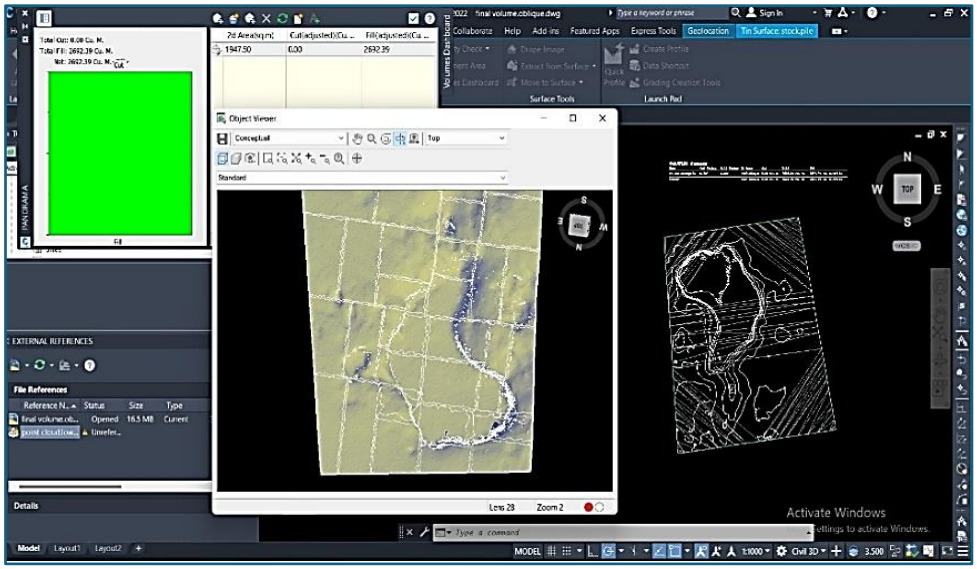

Figure 16. Volume computation from photogrammetric data.

4.3.2 Volume From Fused Data

Following the same logical steps used for calculating volume from UAV photogrammetric data, it was managed to calculate the volume from fused data. The resulting stockpile volume computations from the utilization of the data fusion approach was (2730 m^3) as shown in **Fig. 17**. The accuracy of this volume is affected by the error of co-registration which was

(±35 cm), as shown in **Fig. 18,** and it is considered as one of the limitations in this case study during two reasons clarified above. However, this error is acceptable for earthwork volume estimation projects, but should be managed to overcome for high-accuracy demanding in some construction projects.

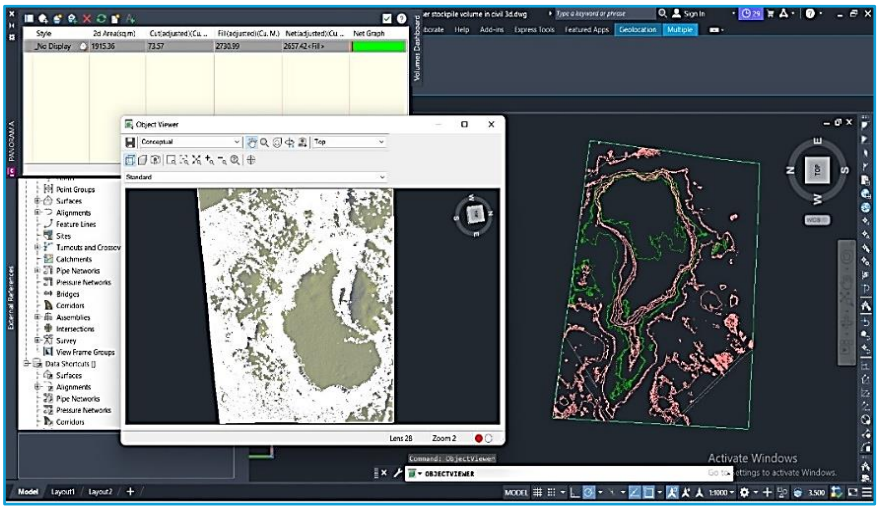

Figure 17. Volume computations from fused data.

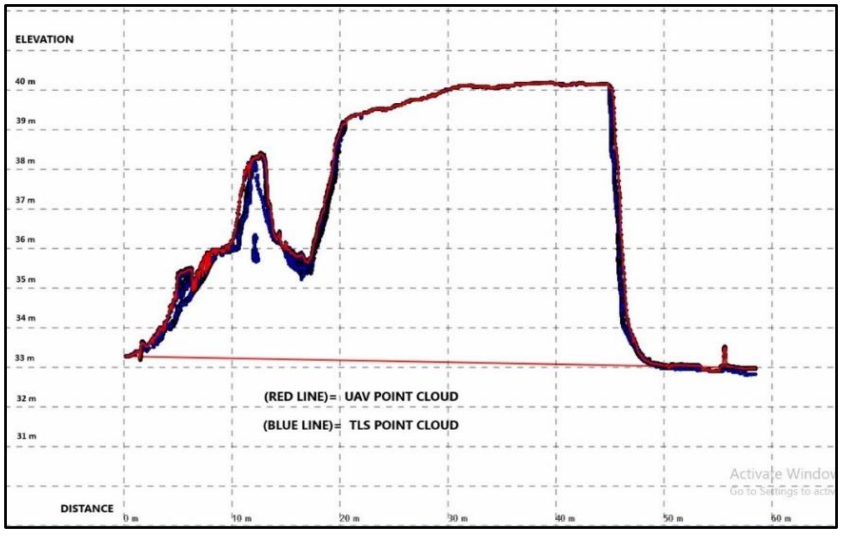

Figure 18. Data profile of UAV photogrammetry and TLS fused datasets showing the co-registration errors. Mismatching is visible between the two points cloud datasets.

4.4 Volume Quality Comparison

In order to judge the estimated volume quality, it is required to rate the data that is used to calculate the volume, and check whether this data obtains the desired details, and accuracy in covering the change in the object surface topography.

The data delivered from the innovative techniques (fused data) covered all sides of the stockpile, represented the complex changes in the object surface topography, and showed a higher quality representation of the OOI. It produced a high level of details, a more realistic representation, and thus provides a more robust approach for volume computations, but it

was noticed that some randomly generated triangles affected the volume calculation process, as shown in **Fig. 19**.

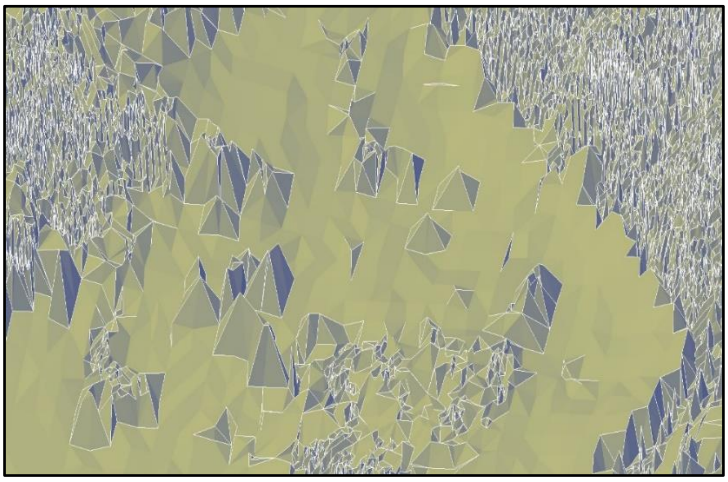

Figure 19. Surface model produced from the fused dataset.

In this study, the volume computations obtained from the UAV photogrammetry standalone dataset have shown the best quality outcomes. The data points extracted from UAV photogrammetry succeeded in describing accurately and smoothly all the details of the stockpile surface including the change in elevation and topography from all sides especially for the top surface of the object which was failed to survey its complete details by TLS technique alone due to the stockpile height, as shown in **Fig. 20**. With regard to accuracy, the UAV photogrammetry volume calculation received the highest degree of confidence, outperforming the fused technique, which was only inferior due to co-registration application restrictions. However, the fusion approach outperforms the photogrammetric approach in handling data occlusions and shadowing problems, better defines surface complexity and edges, increases data enrichment, and also enhances feature detection and Prismoids extraction in 3D space.

Figure 20. Surface model produced from UAV photogrammetry dataset.

4.5 Time Consumption

According to the parameters used and the hardware specifications, image processing took 45 minutes, including alignment and creation of the dense point clouds. It's essential to mention the time spent surveying the GCPs before commencing data collection for all techniques; (9) GCPs were surveyed using GNSS technology, which took (4 hours) for both data collection and processing. For laser scanning technology, it took (11) hours in total, including device setups, data collecting (4 hours), and (2 hours) for scans processing and extracting unified (registration) point clouds. **Fig. 21** illustrates the time consumed for project completion by each technique.

The research execution time may have taken about 20 hours, including fieldwork and office work, following multiple techniques. This is based on average statistical timeline computations of a user having professional skills. However, in this research based on intermediate surveying skills application and elementary photogrammetric and laser skills, this time may be tripled and sometimes expanded to 6X times, including project planning, target establishment, distribution, and technical problem solving.

The UAV data collection took about 14.57 minutes. It is important to take in consideration the time spent to survey the GCPs before starting data collection in both techniques. 9 GCPs were surveyed by using GNSS technology, which consumed approximately 4 hours including data collection and post-processing. Image processing time, including alignment and building dense point clouds, took about 45 minutes according to the settings that were applied and the available hardware specifications. For Laser scanning technology, it took about 4 hours for data collection, 4 hours needed to process the scans, and to extract unified (registered) point clouds. Finally, the time consumed for data collection using the conventional method was about 6 hours, and about 15 minutes for data post-processing. **Fig. 21** shows the time consumption per technique and project execution time percentage.

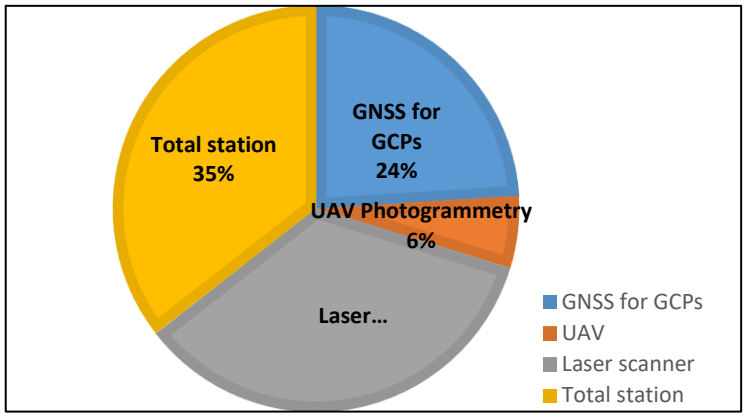

Figure 21. The execution time of the research per technique.

It can be easily noticed from **Fig. 21** that the data collection can be relatively fast using UAV photogrammetry, particularly when applied to small areas. The time spent for the UAV flight varies from a few minutes to an hour based on the complexity of the target area, the OOI size, the image overlap, the accuracy requirements to set gridding coverage, GSD size, and flying height. After data acquisition, images are processed using optimal photogrammetric software, which can consume several hours to multiple days, depending on the number of images and computer processing power. Otherwise, Laser scanning can collect millions of

data points very quickly, usually in a few minutes extends to hours, depending on the area size. However, due to the high-density point clouds, laser scanning data processing time can take several hours, ranging again based on project intricacy.
In contrast, TS surveying is an act of manually measuring distances and angles, which depends on the size and complexity of the project to estimate time consumption. In some cases, especially for simple object size, total station surveying can be quick because measurements can be taken easily and swiftly. However, for complex objects or projects needing a high level of detail, such as volume stockpile computations, it might take days and maybe weeks to provide detailed data. The time consumption for total station surveying also relies on the experience and skill level of the surveying team.

4.6 Instrument Cost Effectiveness

The cost issue is very vital in any engineering project; it clearly outlines to the implementation team the cost headlines of the project budget that they should adhere to the specifying of which materials and equipment also make up the budget and defining the accuracy. Because if a high accuracy is required, then it means a higher cost. The instrument cost of individual techniques utilized in this research is illustrated in **Table 5.**

Table 5. Total instrument cost of individual techniques.

Technique	Cost
GNSS Topcon Gr-5	6750 $
DJI Mini-2	450 $
Stonex X-300 Laser scanner	25000 $

It can be noticed that the cost-effectiveness of the UAV technique (DJI Mini-2) is superior to that of LS (Stonex X-300) and traditional techniques (GNSS Topcon Gr-5 and Total Station Topcon GM-50). The low-cost equipment, therefore, is considered an advantage for the technique, especially for low-budget projects, and it gives a lethal and affordable solution for volume calculation purposes if compared to other available choices. The drone prices could start at $1,000 for basic models and go up to $20,000 or more for professional high end-flying drones with advanced cameras, including the licenses for photogrammetry software, such as Pix4D, Agi-soft Meta shape, which can range from $300 to several thousand dollars for annual subscriptions.
For LS equipment, the TLS prices can start from $ 10,000 going up to over $100,000 for high-end models. Native software for processing point cloud (such as Autodesk Recap, Leica Cyclone) can be expensive too typically in the range of $1,000 to $10,000 or more. However, traditional surveying equipment's cost from $4000 to $7500 for total station depending on the accuracy, and from $5000 to $50000 for high precision GPS system.
To sum up, the results presented are discussing the density, time efficiency, cost effectivity, quality of TIN models and volume comparison between the three adopted techniques. After displaying those elements and discussing the advantages or disadvantages of individual techniques, the outcomes can be summarized the volume quantification results as illustrated in **Table 6** to have a better understanding of volume differences between standalone and integrated modern techniques.

Table 6. Volume results obtained from Individual techniques.

Technique	No. of 3D Point Clouds	Volume m^3	Difference from Traditional	Percentage	Error m.
Photogrammetry (UAV)	863.971	2692.39	+355.71 m^3	+13%	±0.0065
TLS+ UAV	5,592,401	2730.99	+38,6 m^3	+1,5%	±0.35
Traditional (Total Station)	258	3048.10			

5. CONCLUSIONS

This research applied a quantification study to examine the quality of volume calculations obtained from two automatic digital techniques, TLS and UAV-SFM Photogrammetry, in relation to conventional methods. The outcomes led to many conclusions regarding the capability of the individual and integrated data approaches, and showed potential in computing volume. In addition, concluding remarks regarding evaluation analysis were provided based on how long it takes to complete individual techniques and analyze data. The outcomes reflect the potential of remote sensing possibilities by UAV and LS in the measurement of large, irregular-shaped and hard-to-reach objects, specifically material stockpiles and earthwork volume quantification are also included. Multiple conclusions have been derived from this research by utilizing and evaluating the ability of standalone and fusion techniques (i.e. UAV and TLS) to calculate stockpile volumes in construction projects in Iraq:

1. The UAV photogrammetric method is appropriate for volume estimation in earthwork and large irregular stockpiles of various types of materials that are used for construction projects.
2. Low-cost mini-type drones such as (DJI-mini-2) can be used in earthwork volume calculation as applied in this study to discover and assess their potential. It was found out that the 3D model accuracy derived from these drones' data is very potential, comparable to professional drones.
3. Remote sensing techniques give an accurate representation of the object's surface, especially for irregular objects that would be nearly impossible to gain all their details by traditional techniques. This is due to the ability of the UAV and TLS techniques to provide high-density data of the object without missing any details or variations in its surface.
4. When the cost of individual techniques is analyzed, it was found that UAV technique is the most cost-effective technique among those adopted in this study.
5. One of TLS technique limitations is that the resulting point cloud of the object has a gap hole in the top surface due to the inability of the laser beam to reach the top surface of high objects from the ground. As a solution, laser scanner point clouds were combined with UAV point clouds using a pre-planned co-registration approach.
6. The co-registration process accuracy wasn't promising as it had a RMSE of 35 cm, which is considered high, caused by the wrong point target color, which was very difficult to recognize from the background in the registration process. This problem was encompassed by using common targets to register the two-point clouds datasets, but the accuracy was negatively affected. As a matter of fact, this accuracy is considered acceptable for stockpiles or earthwork volume estimation purposes.

7. UAV photogrammetric technique was selected as the preferred technique for stockpile objects volume calculation tasks and that is because of the accurate representation of the object surface, short time needed for data collection, and cost effectiveness. However, combining this technique with a rapid and accurate high-end technique such as TLS is highly recommended to improve volume calculation quality and surface representation realism of the construction stockpile, if reference sphere laser scanning targets are utilized.

Acknowledgement

The authors thank the UOB authorities for granting permission to conduct the field work of this research, including drone reconnaissance and data collection at the study site.

Credit Authorship Contribution Statement

Sharafaddin Th. Muhammed: data collection, methodology implementation, results analysis, data validation, and writing the draft version. Fanar M. Abed: supervision, conceptual and methodological development, data analysis, the practical execution of the study including participation in TLS data collection, and revising and proofreading.

Declaration of Competing Interest

The authors declare that they have no known competing financial interests or personal relationships that could have appeared to influence the work reported in this paper

REFERENCES

Abbas, S.F., and Abed, F.M., 2024. Revolutionizing depth sensing: a review study of apple LiDAR Sensor for as-built Scanning Applications. *Journal of Engineering*, 30(04), pp. 175–199. https://doi.org/10.31026/j.eng.2024.04.11.

Ajayi, O.G., and Ajulo, J., 2021. Investigating the applicability of unmanned aerial vehicles (UAV) photogrammetry for the estimation of the volume of stockpiles, *Journal of Sciendo*, 40(1), pp. 25–38. https://doi.org/10.2478/quageo-2021-0002

Alexiou, E., Viola, I., Borges, T.M., Fonseca, T.A., de Queiroz, R.L., and Ebrahimi, T., 2019. A comprehensive study of the rate-distortion performance in MPEG point cloud compression. *Semantic Scholar*, APSIPA Transactions on Signal and Information Processing, 8(1). https://doi.org/10.1017/atsip.2019.20.

Alkarawi, S.N., and Firas Kh. Jaber, 2023. Integration building information modeling and lean construction technologies in the Iraqi construction sector: benefits and constraints. *Journal of Engineering*, 29(6), pp. 140–158. https://doi.org/10.31026/j.eng.2023.06.11.

Erzaij, K.R., and Obaid, A.A., 2017. Application of building information modeling (3D and 4D) in construction sector in Iraq. *Journal of Engineering*, 23(10), pp. 30-43. https://doi.org/10.31026/j.eng.2017.10.03.

Arango, C., and Morales, C.A., 2015. Comparison between multicopter UAV and total station for estimating stockpile volumes. In: International Archives of the Photogrammetry, *Remote Sensing and Spatial Information Sciences - ISPRS Archives*. International Society for Photogrammetry and Remote Sensing. pp. 131–135. https://doi.org/10.5194/isprsarchives-XL-1-W4-131-2015.

Cucchiaro, S., Maset, E., Cavalli, M., Crema, S., Marchi, L., Beinat, A., and Cazorzi, F., 2020. How does co-registration affect geomorphic change estimates in multi-temporal surveys? *GIScience and Remote Sensing*, 57(5), pp. 611–632. https://doi.org/10.1080/15481603.2020.1763048

Deliry, S.I., and Avdan, U., 2021. Accuracy of Unmanned aerial systems photogrammetry and structure from motion in surveying and mapping: A review. *Journal of the Indian Society of Remote Sensing*, https://doi.org/10.1007/s12524-021-01366-x

Evans, J.S., Hudak, A.T., Faux, R., and Smith, A.M.S., 2009. Discrete return Lidar in natural resources: Recommendations for project planning, data processing, and deliverables. *Remote Sensing*, 1(4), pp. 776–794. https://doi.org/10.3390/rs1040776.

Holz, D., Ichim, A.E., Tombari, F., Rusu, R.B., and Behnke, S., 2015. Registration with the point cloud library: A modular framework for aligning in 3-D. *IEEE Robotics and Automation Magazine, Semantic Scholar*, 22(4), pp. 110–124. https://doi.org/10.1109/MRA.2015.2432331

Janssen, V., 2009. Understanding coordinate reference systems, datums and transformations. *International Journal of Geomatics,* 5(4), pp. 41-53. https://doi.org/10.1201/b17147-4 .

Kovanič, Ľ., Topitzer, B., Peťovský, P., Blišťan, P., Gergeľová, M.B., and Blišťanová, M. 2023, Review of Photogrammetric and Lidar Applications of UAV. *Application Science,* 13(11), *6732.* https://doi.org/10.3390/app13116732.

Lai, J., Mejias, L., and Ford, J.J., 2010. *Airborne vision-based collision-detection system*. [online] *Journal of Field Robotics*, https://doi.org/10.1002/rob.20359

Lukacevic, M., and Füssl, J., 2014. Numerical simulation tool for wooden boards with a physically based approach to identify structural failure. *European Journal of Wood and Wood Products, springer*, 72(4), pp. 497–508. https://doi.org/10.1007/s00107-014-0803-y

Makhathini, T.P., Bwapwa, J.K., Mtsweni, S., 2023. Various options for mining and metallurgical waste in the circular economy: A review. *Sustainability, MDPI, 15*(3), 2518. https://doi.org/10.3390/su15032518.

Malvić, T., Rajić, R., Slavinić, P. and Novak Zelenika, K., 2014. Numerical integration in volume calculation of irregular anticlines. *Rudarsko-geološko-naftnizbornik*, *29*(1), pp. 1-8. https://doi.org/10.2172/4678812

Mohammed, R.A.J., Abed, F.M. and George, L.E., 2015. Improved automatic registration adjustment of multi-source remote sensing datasets. *Journal of Engineering*, *21*(04), pp. 61-81. https://doi.org/10.31026/j.eng.2015.04.04.

Nex, F., and Remondino, F., 2014. UAV for 3D mapping applications: A review. *Applied Geomatics*. https://doi.org/10.1007/s12518-013-0120-x

Nguyen, H.A.D., and Ha, Q.P., 2021. Robotic autonomous systems for earthmoving equipment operating in volatile conditions and teaming capacity. *Semantic Scholar*. https://doi.org/10.1017/S0263574722000339.

Noori, A.M., Al-Saedi, A.S.J., and Abed, F.M., 2024. Optimizing application of UAV-Based SFM Photogrammetric 3D Mapping in Urban Areas. *Iraqi Journal of Science*, 65(5), pp. 2958–2975. https://doi.org/10.24996/ijs.2024.65.5.46

Raeva, P.L., Filipova, S.L., and Filipov, D.G., 2016. Volume computation of a stockpile - A study case comparing GPS and UAV measurements in an open pit quarry. In: International Archives of the

Photogrammetry, *Remote Sensing and Spatial Information Sciences - ISPRS Archives. International Society for Photogrammetry and Remote Sensing*. pp. 999–1004. https://doi.org/10.5194/isprsarchives-XLI-B1-999-2016.

Rashidi, M., Mohammadi, M., Kivi, S.S., Abdolvand, M.M., Truong-Hong, L., and Samali, B., 2020. A decade of modern bridge monitoring using terrestrial laser scanning: Review and future directions. *Remote Sensing, 12*(22), P. 3796, https://doi.org/10.3390/rs12223796.

Remondino, F., 2003. From point cloud to surface: The modeling and visualization problem. *International Archives of the Photogrammetry, Remote Sensing and Spatial Information Sciences*, *34*. https://doi.org/10.3929/ethz-a-004655782.

Salvi, J., Matabosch, C., Fofi, D., Forest, J., and Matabosch, C., 2007. A review of recent range image registration methods with accuracy evaluation. *Image and Vision Computing*, 25(5), pp. 578–596. https://doi.org/10.1016/j.imavis.2006.05.012ï.

Sang, K.K., 2020. Designing material handling system based on volumes extracted using UAV-based photogrammetry. *African Journal of Mining, Entrepreneurship and Natural Resource Management* (AJMENRM). https://doi.org/10.1109/GOL49479.2020.9314754.

Slattery, D.K., and Slattery, K.T., 2010. Evaluation of 3-D laser scanning for construction application. Southern Illinois University Edwardsville Research Report ICT-10-068 https://doi.org/10.1061/(ASCE)SU.1943-5428.0000073

Shanbari, H. A., Blinn N. M., and Issa, R. R. ,2016. Laser scanning technology and BIM in construction management education, *Journal of Information Technology in Construction*, ITcon (21), pp. 204-217.

Shen, N., Chen, L., Liu, J., Wang, L., Tao, T., Wu, D., and Chen, R., 2019. A review of Global Navigation Satellite System (GNSS)-based dynamic monitoring technologies for structural health monitoring. *Remote Sensing,* 11(9), P. 1001. https://doi.org/10.3390/rs11091001.

Tucci, G., Gebbia, A., Conti, A., Fiorini, L., and Lubello, C., 2019. Monitoring and computation of the volumes of stockpiles of bulk material by means of UAV photogrammetric surveying. *Remote Sensing*, 11(12), P. 1471. https://doi.org/10.3390/rs11121471

Turner, D., Lucieer, A., and Watson, C., 2012. An automated technique for generating georectified mosaics from ultra-high resolution Unmanned Aerial Vehicle (UAV) imagery, based on Structure from Motion (SFM) point clouds. *Remote Sensing*, 4(5), pp. 1392–1410. https://doi.org/10.3390/rs4051392.

Viola, P., and Jones, M.J., 2004. Robust real-time face detection. *International Journal of Computer Vision*, https://doi.org/10.1023/B:VISI.0000013087.49260.fb.

Venkataraman, R.R. and Pinto, J.K., 2023. *Cost and value management in projects*. John Wiley & Sons. https://doi.org/10.1002/9780470261033.ch4

Wu, B., Xie, L., Hu, H., Zhu, Q., and Yau, E., 2018. Integration of aerial oblique imagery and terrestrial imagery for optimized 3D modeling in urban areas. *ISPRS Journal of Photogrammetry and Remote Sensing*, 139, pp. 119–132. https://doi.org/10.1016/j.isprsjprs.2018.03.004.

Yakar, M., and Mutluoğlu, Ö., 2010. Close range photogrammetry and robotic total station in volume calculation, *International Journal of the Physical Sciences*, 5 (2), pp. 86-96.

Yakar, M., Yilmaz, H.M. and Mutluoglu, O., 2014. Performance of photogrammetric and terrestrial laser scanning methods in volume computing of excavtion and filling areas. *Arabian Journal for Science and Engineering*, *39*(1), pp.387-394. https://doi.org/10.1007/s13369-013-0853-1

Yulianandha Mabrur, A., Arafah, F., and Sulistianto, A., 2023. Stockpile volume estimation calculation based on terrestrial laser scanner (TLS) data acquisition and 3D surface visualization. *Journal of Applied Geospatial Information (JAGI)*, 7(1), P. 729. https://doi.org/10.30871/jagi.v7i1.4906.

Zhang, J., 2010. Multi-source remote sensing data fusion: Status and trends. *International Journal of Image and Data Fusion*, 1 (1), pp. 5–24. https://doi.org/10.1080/19479830903561035.

الجمع بين المسح الأرضي بالليزر والتصوير الفوتوغرافي المعتمد على الطائرات بدون طيار لتحسين حسابات الحجوم في مشاريع البناء

شرف الدين ثائر محمد*, فنار منصور عبد

قسم هندسة المساحة, كلية الهندسة، جامعة بغداد، بغداد، العراق

الخلاصة

يهدف هذا البحث إلى دمج البيانات المشتركة للقياسات المنتجة من المسح التصويري باستخدام الطائرات الجوية المسيرة *(UAV)* والمسح الليزري الأرضي *(TLS)* لقياسات الحجم لاكداس المواد ذات الأشكال غير المنتظمة المتوفرة في مواقع البناء في العراق. يبحث البحث في إمكانية الجمع بين هذه التقنيات مقارنة بالتقنيات المستقلة والتقليدية لتحسين تحديد الكميات الحجمية واستهلاك وقت اقل. حيث تم اختيار منطقة تحتوي على كومة من المواد السائبة وبقايا المباني. تم استخدام طائرة درون منخفضة التكلفة لجمع البيانات، بينما تم استخدام خوارزميات *Structure from Motion (SFM)* و *Multi View Stereo (MVS)* لمعالجة وتحليل بيانات المسح التصويري. في المقابل، تم استخدام جهاز *Stonex X300 TLS* لجمع بيانات الليزر، بينما تم استخدام برنامج *D Re-constructor* 3 لمعالجة البيانات وتحليلها. الحجم الناتج عن استخدام التقنيات بشكل مستقل جاء على النحو التالي: 2692 متر مكعب من تقنية المسح التصويري للطائرات بدون طيار بدقة تصل الى ±6 ملم، 2730.99 متر مكعب من دمج المسح التصويري والمسح الليزري الأرضي بسيناريو دمج واحد بدقة تصل الى ±35 سم، بينما توفر الطريقة التقليدية 3048 متر مكعب بدقة ±1.1 سم. يُظهر نهج دمج البيانات (الاندماج) مستوى عالٍ من الخطأ بسبب عوائق تسجيل البيانات، والتي يمكن التغلب عليها إذا تم تطبيق نهج التسجيل المستند إلى الهدف لزيادة مستوى الدقة إلى عدة ملليمترات. في هذا البحث، تشير النتائج إلى الفعالية الكبيرة للطائرات بدون طيار منخفضة التكلفة لتقديم قياسات حجم دقيقة في المسح التصويري، والتي تفوق التقنيات التقليدية للتقدير والإدارة والحساب الدقيق لحجم المخزونات والمواد في مشاريع البناء. تمت الموافقة على ذلك من منظور الوقت وكثافة البيانات وفعالية التكلفة وكثافة العمالة بعد تحليل البيانات.

كلمات مفتاحية: أعمال البناء، حسابات الحجم، المخزونات غير المنتظمة، المسح التصويري باستخدام الطائرات بدون طيار، المسح الضوئي بالليزر، تكامل البيانات